ISSN: 2321-3132

Research Article

International Journal of Chemistry and Pharmaceutical Sciences

www.pharmaresearchlibrary.com/ijcps

Single Crystal EPR Studies of Mn (II) Doped in Rubidiumcobalt Sulphatehexahydrate: A Case of Interstitial Location

Hema Ramesh*, S. Sivakumar, M. Rajeswari, A. Rajappa & K. Mageswari

Department of chemistry, Sri Manakula Vinayagar Engineering College, Puducherry,India-605107

Received: 30 June 2014, Accepted: 24August 2014, Published Online: 27 September 2014

Abstract

Electron paramagnetic resonance study of Mn^{2+} ion-doped Rubidiumcobalt sulphatehexahydrate (RCSH) single crystal was carried out at X-band frequency to ascertain its structural properties. EPR spectrum exhibits group of five fine structure transitions each splits into six hyperfine components. The spin Hamiltonian parameters calculated from the crystal rotations are: $g_{xx} = 2.040$, $g_{yy} = 1.986$, $g_{zz} = 1.895$, $A_{xx} = 10.25$ mT, $A_{yy} = 8.85$ mT, $A_{zz} = 8.46$ mT, $D_{xx} = 16.68$ mT, $D_{yy} = -5.93$ mT, $D_{zz} = -10.74$mT, $E = 8.09$ mT. The detailed study revealed that only one site was present in the lattice interstitially. From the observed spin Hamiltonian parameters, it was concluded that the site symmetry around the central metal ion was a compressed octahedral with rhombic symmetry. EPR spectra of Mn(II) doped in had been done at room temperature. The direction cosines obtained from the single crystal rotation spectra showed that the paramagnetic impurity had entered the lattice interstitially. The distortion from axially symmetry for the paramagnetic impurity was noticed, especially in zero-field terms and confirmed the orthorhombic nature of Mn (II). From the Matumura's plot, the complex was found to be ionic in nature. Further studies are planned to calculate spin relaxation with varying temperatures. FTIR and Powder XRD spectra supported to evaluate lattice parameters within the dopant.

Keywords: spectrum, Hyperfine, orthorhombic symmetry, Hamiltonian parameters, interstitial.

Contents

***Corresponding author**
Hema Ramesh
Department of chemistry,
Sri Manakula Vinayagar Engineering College, Puducherry, India-605107
Manuscript ID: IJCPS2188

PAPER-QR CODE

1. Introduction

Single crystal EPR studies of Mn (II) ion in Tetraaquabis (hydrogen maleato) cadium (II) [1], Cu(II) and VO(II) doped in diaqua(2,20-bipyridine) malonato zinc(II) complex were reported [2,3]. The results shown that incorporated paramagnetic ion was entered the lattice interstitially, due to the structural constraints. Transition metal ion-doped crystals are useful for laser and optical fibre applications because of their spectroscopic behaviours[4]. The transition

metal ions are responsible for modification of many physical properties and play a major role in devices such as wave-guides, holography and electro-optical devices [5]. Since these applications, the growth and characterization of transition metal ion-doped complexes has become important area of research. There are many enzymes and proteins are found in biological systems in which Mn(II) is an active centres [6–8], so understanding of Mn(II) by EPR is significant. The probability of getting information about symmetry and structure from magnetically concentrated systems is narrowed because of very broad resonance in EPR, arising due to the presence of electron dipole–dipole and exchange interactions. Hence, to study the symmetry around embedded ion and covalence, paramagnetic ions should be incorporated into diamagnetic host lattices. When the paramagnetic ions are doped into diamagnetic host, local symmetry distortion arises because of the difference in the size of the doped ion and that of the host ion. Electron paramagnetic resonance (EPR) also known as electron spin resonance (ESR) is an important spectroscopic tool for the study of paramagnetic defects in solids. EPR studies are usually carried out by doping paramagnetic impurities in diamagnetic hosts to obtain well resolved spectra due to the minimization of dipolar and exchange phenomenon. On the other hand, the use of paramagnetic host for EPR studies has its own drawbacks since the resonance lines of the impurity get broadened due to dipolar between the host and impurity ions. However, many systems of different transition metal ions doped with paramagnetic hosts are studied by EPR spectroscopy.

These give information about dopant, spin Hamiltonian parameter technique and structural parameters. Additionally EPR can be extensively used to study the structural phase transitions in crystals since the magnitude and orientation of zero-field splitting tensor is highly sensitive to the strength and geometry of the crystal field [9,10]. The problem of the exact site occupancy can be determined by the spectroscopic techniques and among these, EPR is an appropriate tool, since this technique is most sensitive to local symmetry, the character of chemical bonds as well as to other structural factors. Similar EPR studies can, in principal, be carried out by incorporating paramagnetic ions in paramagnetic hosts. The study of EPR spectra of paramagnetic ions in paramagnetic hosts will provide additional information, besides that obtained from the diamagnetic hosts.

Therefore, a comparison of EPR spectra of isomorphous diamagnetic and paramagnetic hosts provides interesting and important information regarding the line widths, g-values and the magnetic interactions between the dopant and the host ions. In these paramagnetic hosts, the effect of dipolar interaction is reduced either by 'spin-quenching' or by motional effects [11-16]. The spin-quenching produces sharp spectra by a reduction of the individual magnetic moments of the host ions. Past few years our research group concentrating on single crystal EPR studies of paramagnetic metal ions doped Tutton's salts as they are very interesting systems having two divalent and monovalent cations. They also provide very fascinating information like spin relaxation etc [17-21]. In the paper, we have reported here Mn (II) doped Rubidium Cobalt Sulphate Hexahydrate (hereafter abbreviated as RCSH). Among the transition metal ions, divalent manganese have been selected since the shell contains five unpaired electrons (S =5/2) with half filled configuration and resultant angular moment is zero. The ground state of Mn (II) is $^6S_{5/2}$. EPR studies of Mn (II) are done quite expansively in the exploration of structural and dynamic aspect of crystalline state since zero field splitting in these ions are sensitive to even small distortions. The study is further widened to ascertain the location of Mn (II) present in RCSH and find out the spin Hamiltonian parameters, predict distortion, relaxation and bonding parameters.

2. Crystal structure

Tutton's salts have the general formula $M"M_2'(XO_4)_2.6H_2O$, where M" is a divalent cation like Co, Cu, Ni, Mg, Zn; M' is a monovalent cation like K, Cs, Rb, NH_4 and X is S or Se. Tutton's salts have monoclinic crystal structure with space group $P2_{1/n}$. The lattice parameters of RCSH (M" is Co, M' is Rb and X is S) are: a = 0.613, b = 1.223, c = 0.909 nm, β = 104.78º and Z = 4 [22]. The structural data indicates that the central cobalt ion is surrounded by six water molecules in the form of a compressed octahedron. However, in most of the Tutton's salts, the shortest Co-O bond is fixed, whereas the longest bond depends on the nature of M' and M". The structure of RCSH is given in Fig.1. From the X-ray data of the host lattice, the direction cosines of the three Co–O bond directions were calculated and given in Table.1.

Table1: Direction cosines of the three Co–O bond directions and that of the distortion axis, calculated from the procedure given in text.

	Direction cosines		
M-L bond	a	b	c*
Co-O(1)	0.000	-0.8902	0.4556
Co-O(3)	-0.7314	-0.3344	0.5944
Co-O(4)	-0.7143	-0.3265	-0.6190

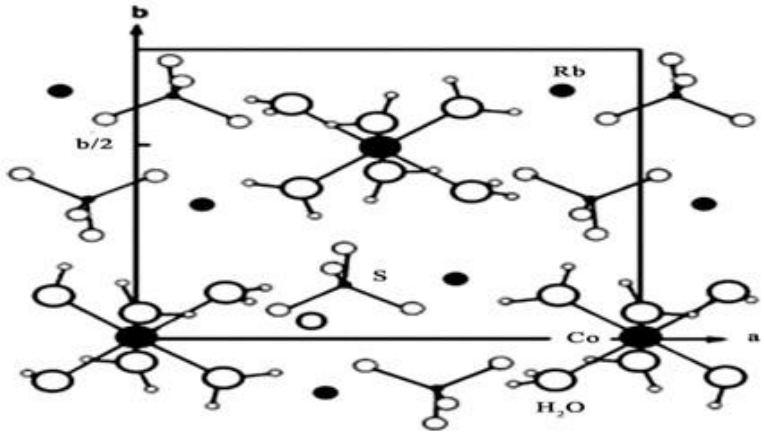

Figure 1: Single Crystal XRD Structure of Rubidiumcobaltsulphatehexahydrate (RCSH) (19)

3. Experimental

3.1. Preparation of Mn^{2+} doped RCSH crystals

Single crystals of Mn(II) doped Rubidium Cobalt Sulphate Hexahydrate, $CoRb_2(SO_4)_2 \cdot 6H_2O$ were grown by slow evaporation of an equimolar aqueous solution of Rubidium sulphate and Cobalt sulphate. To this 0.1% of the paramagnetic impurity was added in the form of manganese (II) chloride. Good red coloured single crystals were obtained within 15 days.

3.2. UV, FT-IR, powder XRD measurements

Optical absorption spectrum was recorded at 300 K using a Varian Cary 5000 Ultraviolet (UV–Visible) near infrared spectrophotometer in the range of 200–800 nm. FTIR spectra were recorded for doped and undoped crystals on a Shimadzu FTIR -8300/8700 spectrometer in the range of 4000–400 cm^{-1}, using almost transparent KBr pellets containing fine powder sample at 300 K. Powder XRD studies were carried out at 300 K for doped and undoped materials on a PANalytical X'pert PRO diffractometer with Cu Kα radiation of wavelength 0.15406 nm and 2θ range between 5 and 75°.

3.3. EPR measurements

EPR spectra were recorded at 300 K on a JEOL JES –TE100 ESR spectrometer operating at the X-band microwave frequency, equipped with 100 kHz field modulation for obtaining first derivative EPR spectrum. DPPH with a g value of 2.0036 is used for g-factor calculations. Angular variations are made by rotating the crystal along the three mutually orthogonal axes a*, b, c* in 10° interval. Isofrequency plots of each plane were simulated using the EPR-NMR program [23].

4. Results and discussions

4.1. *UV-Visible, FTIR, and powder XRD studies of Mn(II) doped RCSH*

The spectrum exhibited five bands at 840, 673, 543, 349 and 269 nm. Fig.2a shows characteristic features of Mn(II) in octahedral symmetry. The absorption bands at 11 904, 14 849, 18 391, 28 653 and 37 164 cm^{-1} were in the order of d-d transition of manganese (II) ion. From the nature and position of the band observed, these bands were attributed to Mn(II) in distorted octahedral symmetry. The first one is the CT band and remaining four bands were assigned to $^6A_{1g}(S) \rightarrow {}^4T_{1g}(G)$, $^6A_{1g}(S) \rightarrow {}^4E_g(G)$, $^6A_{1g}(S) \rightarrow {}^4E_g(D)$, $^6A_{1g} \rightarrow {}^4A_{1g}(G)$ transitions respectively, with the help of Tanabe Sugano diagram. The energy matrices for the d^5 configuration inclusive of trees correction were given by Mehra. In the analysis of optical absorption spectrum, trees correction parameter was included in addition to the crystal field parameter Dq and Racah interaction parameters B and C. The values were the best fit with observed data are Dq = 820, B = 857 and C = 2932 cm^{-1}. The band data were well matched with reported literature. The value of the interelectronic repulsion parameter B (837 cm^{-1}) obtained in the present work, when compared with the free ion value (960cm^{-1}) decreased by an amount of 13%. This decrease was caused by influence of bond covalency.

The FT-IR spectrum of RCSH and Mn(II) doped RCSH were recorded at room temperature and illustrated in Fig.2b. The FT-IR spectrum of RCSH showed characteristic bands for -OH, OH_2, COO-, $-CH_2-$ and Co-O. FT-IR spectrum of Mn(II) doped RCSH also showed comparable characteristic bands with RCSH and slight wave number shift observed due to low concentration of Mn(II) impurity. The observed FT-IR bands and their tentative assignments for RCSH and Mn(II) doped RCSH are depicted in Table.2. The powder XRD pattern of Mn(II) doped RCSH was recorded at room temperature and presented in Fig.2c. Lattice parameter also calculated along with single crystal data of RCSH are listed in Table.3. According to the powder XRD measurements, the Mn(II)/ RCSH had the identical lattice parameters as the pure RCSH, this clearly indicated that paramagnetic impurity did not alter the

structure of RCSH due to low concentration of Mn(II) impurity.

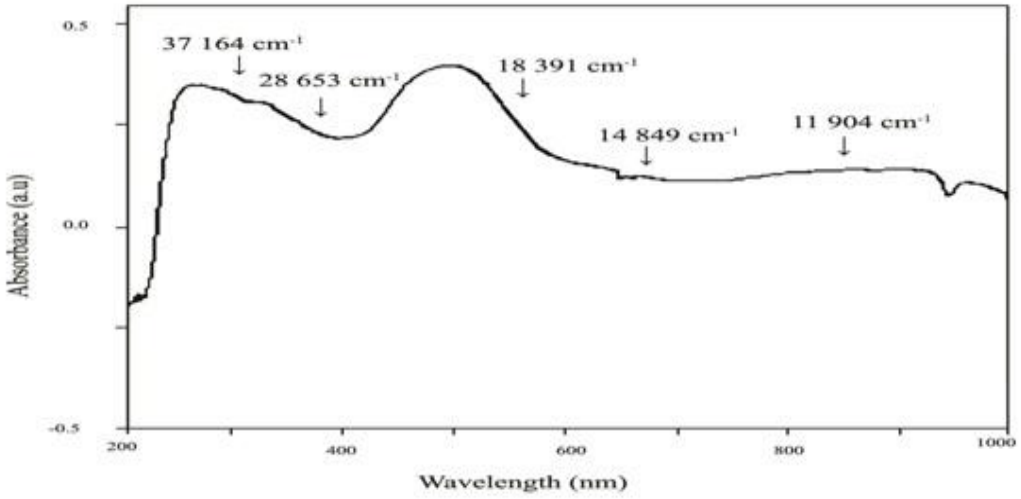

Figure 2a: Optical spectrum of Mn(II)/ RCSH, recorded at room temperature

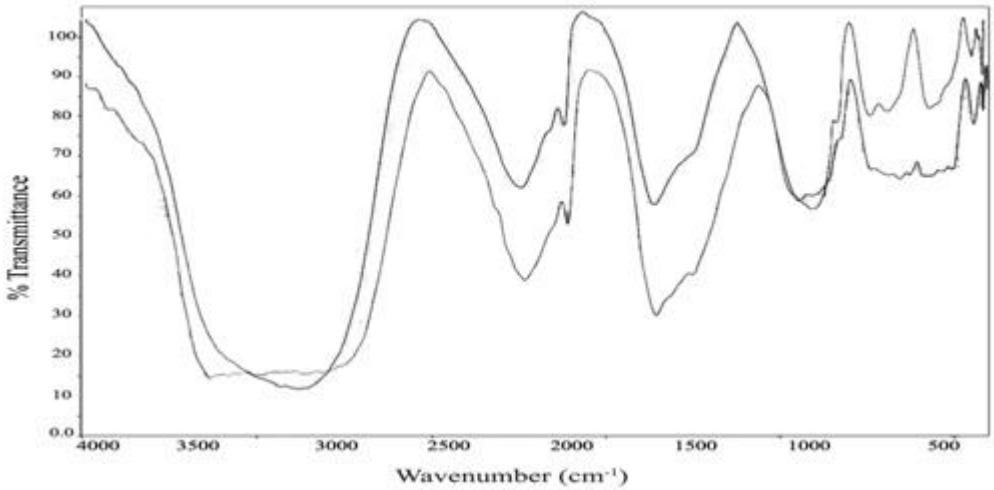

Figure 2b: FT-IR spectra of pure (top) and Mn(II) doped RCSH (bottom) at room temperature

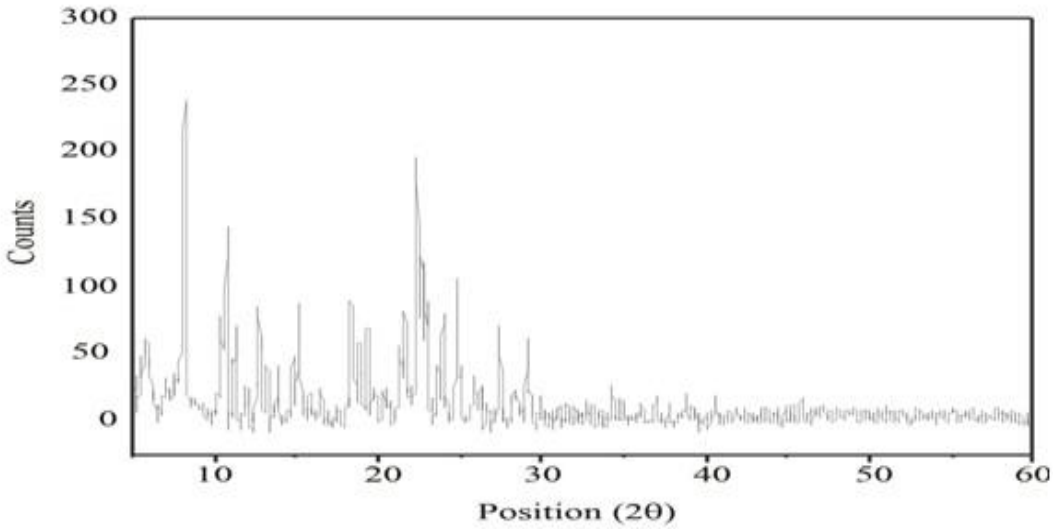

Figure 2c: Powder XRD pattern of Mn(II) doped RCSH

Table 2: Observed FT-IR bands and their tentative assignments for RCSH and Mn(II) doped RCSH

Assignments	**RCSH (cm^{-1})**	**Mn (II) / RCSH (cm^{-1})**
Co-O	912, 572	932
(C = O) + (C – H)	1588	1591
OH_2	3246, 3105	3838, 3118
$-CH_2$	1184, 2851	1192, 2859
-OH	3471, 3874	3469, 3661

Table 3: The calculated lattice parameters of RCSH and Mn(II)-doped RCSH from powder XRD, along with single crystal XRD of RCSH

Lattice parameter (nm) of RCSH from single crystal XRD	**Lattice parameters (nm) calculated from powder XRD**	
RCSH	RCSH	Mn(II) doped RCSH
a = 0.613	a = 0.618	a = 0.6209
b = 1.223	b = 1.1096	b = 1.1085
c = 0.909	c = 0.9108	c = 0.9202

4.2. EPR studie

A single crystal EPR spectrum was carried out at ambient temperature for Mn(II) doped RCSH. A good single crystal was mounted and typical EPR spectrum was obtained when the external magnetic field (B) was parallel to the crystallographic a –axis as shown in Fig.3a. It consisted of 30 line hyperfine patterns. Manganese has the $3d^5$ electronic configuration having five unpaired electron in the out most shell. In the absence of applied magnetic field, the ground state of Mn(II) ion ($^6S_{5/2}$) splits into three Kramers doublets, due to spin–spin interaction, with separations of 4D and 2D. These Kramers doublets split further, by the application of external magnetic field, into six levels. Transitions between these six levels will give rise to five equally spaced lines, each of which further splits into a sextet due to hyperfine interaction resulting from the nuclear spin of ^{55}Mn (I = 5/2).

During the crystal rotation all the three planes almost gave thirty lines pattern with anisotropy. EPR spectra which were obtained, when applied magnetic field was parallel to b axis and c* axis were given in Figs.3a and 3b. During single crystal rotations, variation in hyperfine resonance positions in ac* and ab planes was noticed. In order to obtain spin Hamiltonian parameters for Mn(II)/RCSH, crystal rotations were performed in the two mutually orthogonal planes, and the isofrequency plots for bc* and ab planes are given in Figs.4a-4b respectively. Even though the unit cell contains Z = 4, only one site was observed for all the two planes during the crystal rotation. In the two angular variation planes the solid lines represent experimental values whereas solid points represent hypothetically calculated ones. A good agreement was achieved.

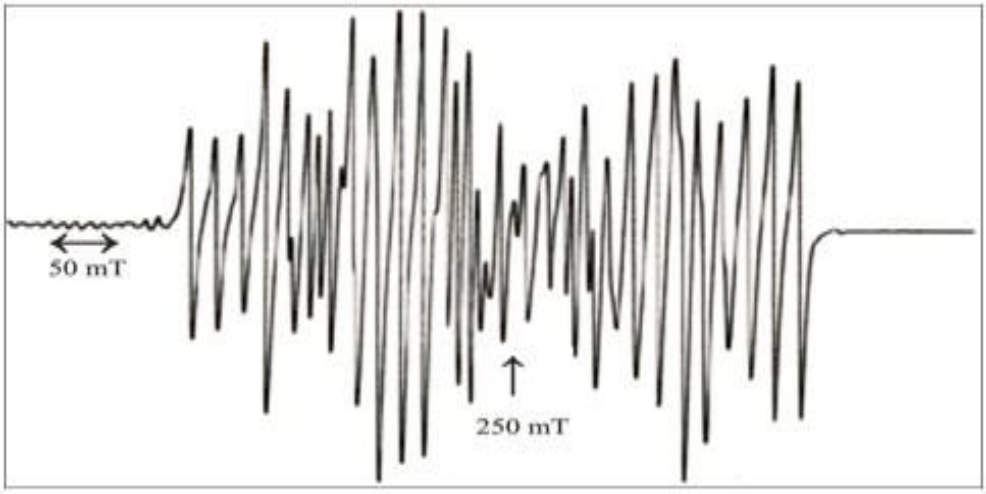

Figure 3a: Single crystal EPR spectrum of Mn (II)/ RCSH, when, the applied magnetic field (B) is parallel to c* axis in ac* plane. Frequency =9.06036 GHz.

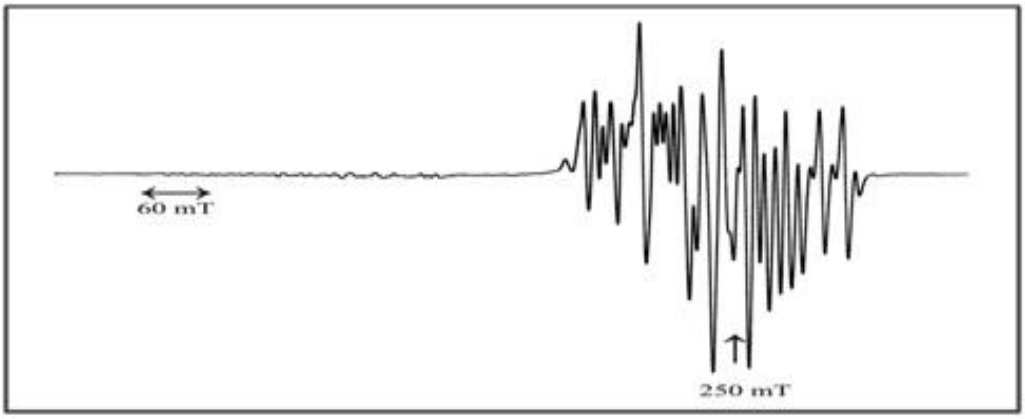

Figure 3b: Single crystal EPR spectrum of Mn(II)/ RCSH, when applied magnetic field (B) is parallel to b axis in ab plane. Frequency =9.05932 GHz

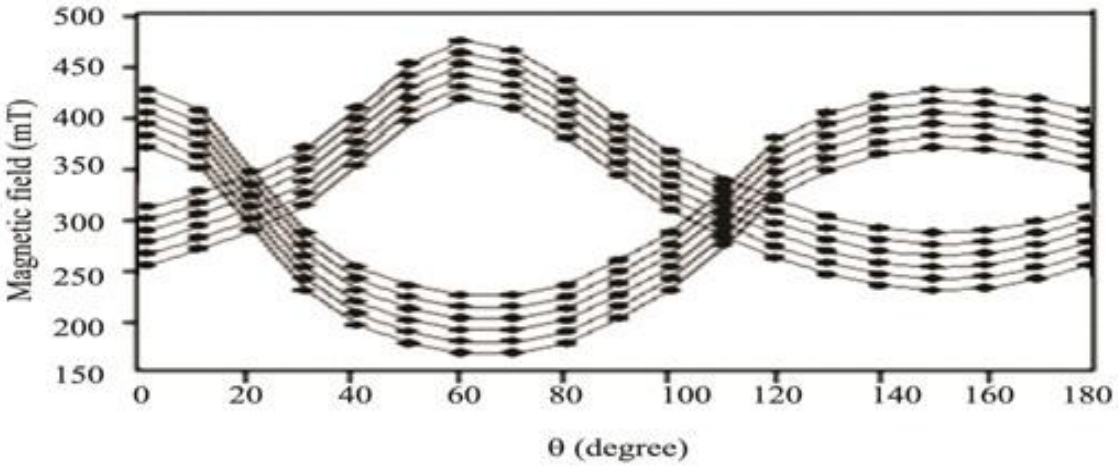

Figure 4a: Angular variation plot of Mn(II) doped RCSH in the bc* plane. Frequency = 9.06036 GHz

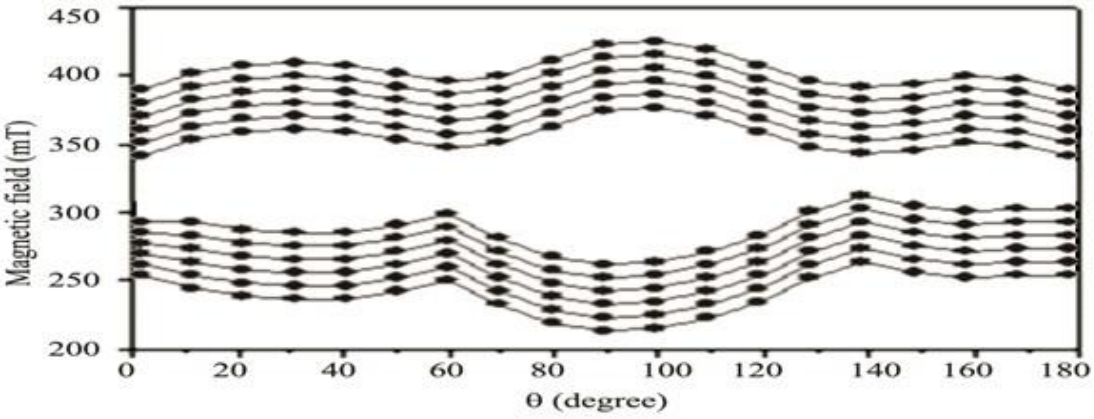

Figure 4b: Angular variation plot of Mn(II) doped RCSH in the ab plane. Frequency = 9.05932 GHz.

4.3. Calculation of Spin Hamiltonian Parameters

The angular variation of the Mn(II) hyperfine resonances in the three planes were successfully fitted to the following spin Hamiltonian using EPR–NMR (Nuclear magnetic resonance) program to find spin Hamiltonian parameters (including second order effects).

$$\mathcal{H} = g_{xx}\beta B_x S_x + g_{yy}\beta B_y S_y + g_{zz}\beta B_z S_z + A_{xx}S_x I_x + A_{yy}S_y I_y + A_{zz}S_z I_z + D\left[S_z^{\,2} - \frac{1}{3}S(S+1)\right] + E\left[S_x^{\,2} - S_y^{\,2}\right]$$

where first term is the Zeeman energy, and the second term is due to hyperfine interaction. The axial and rhombic components of the zero fields splitting are represented by the third and fourth terms. S_x, S_y, S_z are the spin operators with respect to the cubic field axes. The parameters D and E are zero fields splitting due to rhombic and axial crystalline field matrix and E represents the deviation from the axial symmetry. Using the above equation, calculated spin Hamiltonian parameters are shown in Table.4 along with respective direction cosines. Table.4 clearly indicates that g/A/D are nearly coincident, and additional geometry of Mn(II)/RCSH is distorted octahedral symmetry. The value of D is relatively higher than observed from normal Mn(II) complexes. In order to classify the position of the Mn(II)/RCSH, the direction cosines of various Co-O bonds are calculated from X-ray data and given in Table.5, which shows the direction cosines of g/A values did not match with direction cosines of cobalt oxygen bonds obtained from crystallographic data. Also, it indicates the paramagnetic transition metal ion namely Mn(II) ion was present in the lattice interstitially.

The road maps were simulated for both the planes and agreed well with the experimental ones.The spin Hamiltonian parameters observed from single crystal analysis were further confirmed by taking polycrystalline EPR spectrum. The powder EPR spectrum of Mn(II)/ RCSH is shown in Fig.5. The calculated spin Hamiltonian parameters were: g = 2.0078, A = 9.6 and D = 52.24 mT. These values were almost close to those parameters acquired from single crystal analysis. The powder EPR spectrum was simulated using these values which confirm the accuracy of the evaluated spin Hamiltonian parameters shown in Fig.5. The spin Hamiltonian parameters obtained for Mn(II) doped RCSH are summarized in Table.5 along with similar results of earlier works for comparison. [22,24,25].

Table 4: Spin-Hamiltonian parameter matrices (g, A and D) calculated from the iso-frequency plots in the three planes, using EPR–NMR program [22]

	Eigen values			**Direction Cosines**		
				a	b	c*
g matrix						
	1.965	0.073	1.986	-0.9903	-0.0092	-0.1383
		1.974	1.895	-0.0881	-0.7282	0.6796
A matrix (mT)						
8.82	-0.10	0.100	10.25	0.0669	0.0386	0.9970
	8.49	0.070	8.850	-0.9583	0.2806	0.0535
		10.24	8.460	-0.2777	-0.959	0.0558
D matrix (mT)						
-6.15	0.96	0.300	16.68	-0.0063	-0.4358	0.8999
	-5.36	-10.67	-5.930	-0.9772	-0.1881	-0.0982
		11.51	-10.74	0.2121	-0.8801	-0.4247

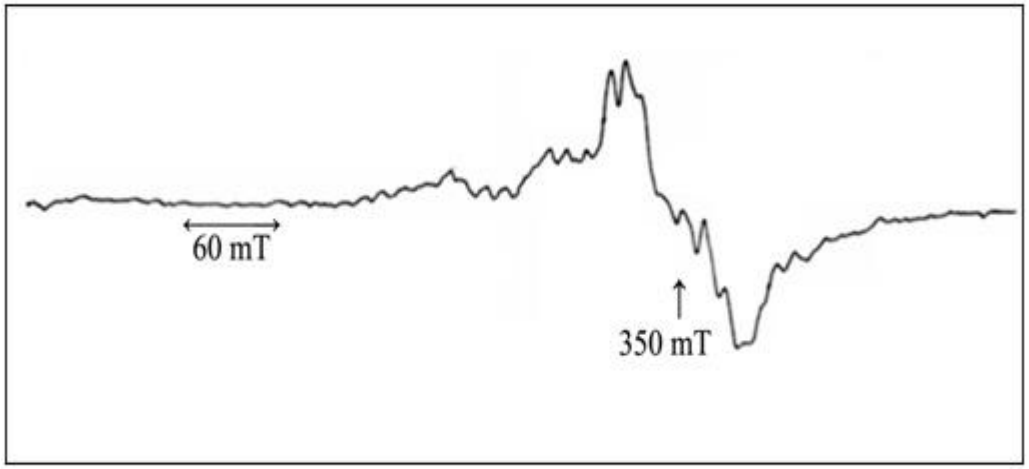

Figure 5: Powder EPR spectrum of Mn(II) doped RCSH is recorded at room temperature. Frequency: 9.03595 GHz.

Table 5: Spin Hamiltonian parameters for Mn(II) in RCSH and few related host lattices

System	g	A	D	Reference
RCSH	2.040	10.25	16.68	
	1.986	8.85	-5.93	Present case
	1.895	8.46	-10.74	
MRSH	1.974	8.58	-18.71	
	1.980	9.87	-5.59	19
	1.961	9.24	24.30	
ZMTH	2.010	8.7		
	1.992	8.7	36.5	20
	2.035	8.7		
NMTH	2.030	-8.40		
	2.008	-8.90	22.3	21
	1.980	8.20		

RCSH Rubidiumcobaltsulphatehexahydrate
MRSH Magnesium Rubidium Sulphate Hexahydrate
ZMTH Zinc Maleatetetra Hydrate
NMTH Nickel MaleateTetraHydrate

4.4. Covalency of metal ligand bonds

The covalency of the bond between manganese and oxygen's ligand can be calculated using Matumura's plot [26]. The covalency of a bond between manganese and its ligands depends on the magnitude of the isotropic hyperfine coupling constant" A". An approximate relationship for the covalency of a bond between the atom p and q and their electro negativities χ_p and χ_q is given below

$$C = [1 - 0.16(\chi_p-\chi_q)-0.035(\chi_p-\chi_q)^2]/n$$

Where, n is the number of neighboring atoms surrounding the Mn(II) ion. Using the values $\chi_{Mn} = 1.55$ and $\chi_{O} = 3.44$, (Pauling's scale) and the percentage of covalency obtained in our case in the above equation was 8.2%, indicating that compound was almost ionic nature. Also, the covalency of the bond between manganese and its ligands influenced the magnitude of the isotropic hyperfine coupling constant. The hyperfine coupling constant A obtained from Matumuras's plot matched well with the calculated value.

5. Conclusions

Single crystal EPR studies of Mn(II) doped RCSH carried out at room temperature show 30 line pattern indicating the presence of single site in the crystal structure. The spin Hamiltonian parameters (g, A, D) were calculated. The spin relaxation time was calculated from line width of Mn(II) and found to be comparable to the value reported for other cobalt complexes. Optical spectra was used to find Racah parameter and FTIR helped to identify host lattice. Powder XRD was employed to calculate the lattice parameters; which clearly show that the lattice formed is RCSH. The spin relaxation studies are planned.

6. Acknowledgements

The authors thank the Dr.P. Sambasiva rao (late) and also thank CSIR and DST for financial assistance.

7. References

1. S. Ramachitra, R. Hema, P. Muthuausteria, K. Parthipan, J. Mol.struct. **2014**, 1058: 173-180.
2. K. Parthipan, P.S. Rao, J. Mol. Struct. **2010**, 977: 130.
3. K. Parthipan, R. Hema, P.S. Rao, J. Mol. Struct. **2011**, 992: 59-64.
4. S. Kück, Appl. Phys. **2001**, 72 B: 515-562.
5. W.C. Zheng, Phys. Status Solidi B. 205 (1998) 627.
6. A. Gelasco, M. Baldwin, V.L. Pecoraro, in: H.H. Thorp, V.L. Pecoraro (Eds.), A ModellingApproach For Understanding the Mechanism of Manganese Enzymes in Mechanistic Bioinorganic Chemistry, Adv. Chem Series, ACSBooks, Washington, D.C., **1995**, p. 265.
7. P. Chelikani, I. Fita, P.C. Loewen, Cell. Mol. Life Sci. 61 (2004) 192–208.
8. S.L. Marklund, N.G. Westman, E. Lundgren, G. Roos, Cancer Res. 42 (1982) 1955–1961.
9. F.J. Owens, Magnetic Resonance of Phase Transitions, Academic Press, New York, (1979).
10. R. Murugesan, S. Subramanian, J. Magn. Reson., 57 (1984) 385.
11. R. Kubo, K.Tomita, J. Phys. Soc. Japan., 9 (1954) 888.
12. A.K. Jain, G.C. Upreti, J. Phys. (C): Solid State Phys., 13 (1980) 5177.
13. J. Lech, A. Siezak, R. Hrabanski, J. Phys. Chem. Solids., 52 (1991) 685.
14. R. Murugesan, A. Thamarai Chelvan, A. Milton Franklin, V. Ramakrishnan, Mol. Phys., 79 (1993) 663.

15. K.V. Narasimahulu, J. Lakshmana Rao, Physica B., 37 (1998) 254.
16. T. Jeyabalan, P. Sami, A. Shunmugasundaram, R. Murugesan, Spectrochim. Acta. 55A (1999) 2187.
17. H. Anandalakshmi, K. Velavan, I. Sougandi, R. Venkatesan, and P. Sambasiva Rao, Pramana., 62 (2004) 77.
18. H. Anandalakshmi, I. Sougandi, K. Velavan, R. Venkatesan, and P.Sambasiva Rao, Spectrochim. Acta., A 60 (2004) 2661.
19. S. Boobalan, P. Sambasiva Rao, J. Organo. Chem., 695 (2010) 963.
20. S. Boobalan, P. Sambasiva Rao, Radiat. Eff. Defects Solids., 28 (2010) 1.
21. K. Kannan and M. A. Viswamitra, Z. Kristallogr., 60 (1965) 122 .
22. B. Sankar, B. Natarajan, H. Anadhalakshmi, P. Sambasiva Rao, Crysl Res. Technol., 2 (2007) 173.
23. F. Clark, R.S. Dickson, D.B. Fulton, J. Isoya, A. Lent, D.G. McGavin, M.J. Mombourquette, R.H.D. Nuttal, P.S. Rao, H. Rinnerberg, W.C. Tennat, J.A. Weil, EPR –NMR program, University of Saskatchewan, Saskatoon, Canada, 1996.
24. M. Vital, R. Jaganathan, J. Chem. Soc. Daltan Trans., (1988) 983.
25. N. O. Gopal, K. V. Narasimhulu, J. L. Rao, Journal of Phys. Chem Solids., 63 (2002) 295.
26. O. Matamura, J. Phys. Soc. Jpn., 14 (1959) 108.